The magnetic transition in Fe-substituted hexagonal β-Al_9SiMn_3

1990 J. Phys.: Condens. Matter 2 3855

(http://iopscience.iop.org/0953-8984/2/16/014)

J. Phys.: Condens. Matter 2 (1990) 3855–3865. Printed in the UK

The magnetic transition in Fe-substituted hexagonal β-Al_9SiMn_3

R A Brand†, G Le Caër‡, J-M Dubois‡, F Hippert§, C Sauer† and J Pannetier‖

† Institüt für Festkörperforschung der KFA Jülich, Postfach 1913, D-5170 Jülich, Federal Republic of Germany

‡ Laboratoire de Science et Genie des Materiaux Metalliques (CNRS UA 159), Ecole des Mines, F-54042 Nancy Cédex, France

§ Laboratoire de Physique des Solides, Université de Paris Sud, F-91405 Orsay Cédex, France

‖ Institute Laue–Langevin, Boite Postale 156X, F-38042 Grenoble Cédex, France

Received 12 July 1989, in final form 28 November 1989

Abstract. Pure hexagonal β-Al_9SiMn_3 does not order magnetically down to at least T = 4.2 K. Recently we have studied β-$Al_9Si(Mn_{1-x}Fe_x)_3$ using Mössbauer effect spectroscopy with $x = 0.28$ (1987 *Phil. Mag. Lett.* **56** 143–51) and discovered a new transition at about 80 K. Here we present neutron diffraction studies down to 5 K, which reveal no structural changes, so that this transition at 80 K is indeed of magnetic origin. The magnetic susceptibility on the alloy with this Fe concentration shows evidence of a small maximum near this temperature superimposed on a large Curie-like background. The height of this maximum above the background is consistent with an antiferromagnetic transition at this temperature involving mainly the Fe moments. In addition to this transition, the Curie-like background shows a strong maximum (cusp) near 4 K. We thus infer a magnetic double transition in this disordered alloy. The upper transition at $T_C = 80$ K involves mainly Fe moments. The lower transition at $T_g = 4$ K is spin-glass-like, and must involve both Mn and Fe moments. These magnetic transitions have been followed to lower Fe concentrations ($x = 0.10$ and 0.20) by both Mössbauer spectroscopy (T_C) and by magnetic susceptibility (T_g). It is found that T_C decreases rapidly with decreasing Fe concentration, while T_g remains relatively constant. The saturation hyperfine field $B_{hf}(0)$ decreases rapidly with decreasing x, indicating that the Fe atoms lose their magnetic moments in the limit of infinite dilution, and the important role played by Fe–Fe nearest neighbours in determining the magnetic properties.

1. Introduction

The hexagonal compound β-$Al_{10-x}Si_xMn_3$ [1], henceforth referred to as β-Al_9SiMn_3, has attracted some interest because of the possible proximity of this crystal structure to the icosahedral quasi-crystal (QC) with composition near to i-$Al_{85}SiMn_{15}$ [2]. In the hexagonal phase, there is only one Mn site, and two Mn nearest neighbours per Mn atom [1]. The hexagonal crystal structure of the idealised metastable end-member (no

0953-8984/90/163855 + 11 $03.50

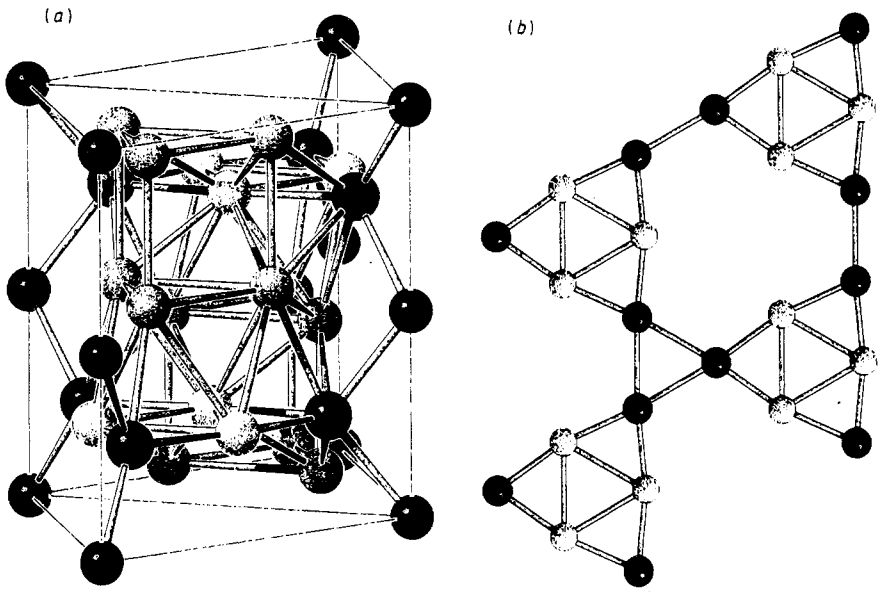

Figure 1. The lattice structure of the ideal β-Al_9SiMn_3. (*a*) In perspective, the Al atoms in 'grey', and the Mn atoms in 'black'. (*b*) Cut showing the first and second Mn NN.

silicon) $Al_{10}Mn_3$ given by Taylor [3] is shown in figures 1(*a*) and (*b*). Figure 1(*b*) shows a projection of the Mn–Mn two first nearest neighbours (NN) at 2.682 Å and the four second NN at 4.156 Å. The first NN form groups of triplets. It is known that β-Al_9SiMn_3 does not order magnetically but has a small temperature-independent paramagnetic susceptibility ($\chi = 3.3 \times 10^{-8}$ m^3 kg^{-1}) at least down to 4.2 K [4]. On the other hand, i-$Al_{74}Si_6Mn_{20}$ shows a Curie–Weiss-like susceptibility with an average effective moment per Mn atom of about 1.3 μ_B [4, 5] and a spin-glass transition at low temperatures ($T_g \simeq$ 5 K) [4]. It was shown by Warren *et al* [6] that the Mn sites in the icosahedral quasi-crystal can be separated into two different groups, the majority being non-magnetic, and a minority (of about 15%) being magnetic. This result has led to speculation that the non-magnetic sites in i-$Al_{74}Si_6Mn_{20}$ must be similar to the Mn site in non-magnetic β-Al_9SiMn_3. This has been at least indirectly confirmed by our recent in-field Mössbauer studies [7, 8], in which we showed that, among the different Al–Si–Mn crystalline phases, only the hexagonal phase has a similar sign and magnitude of the electric field gradient (EFG). In addition, Warren *et al* [6] have suggested that the magnetic properties of the i-$Al_{74}Si_6Mn_{20}$ quasi-crystals are related to the inherent disorder of this non-periodic structure.

Hauser *et al* [9] have reported on ferromagnetic order in amorphous Al–Si–Mn alloys in the limit of 25–30 at.% Si. They also report on a ferromagnetic transition in a crystallised alloy in the same range of silicon content. They have denoted this as the β-structure, but there is no evidence that, in fact, these samples were in the hexagonal phase, and the range of silicon content is much larger than the 4–8 at.% usual for this compound [1]. Recently, Dunlap *et al* [10] have found ferromagnetic-like behaviour in both amorphous and quasi-crystalline $Al_{80-y}Si_yMn_{20}$ alloys with $y = 25$ and 30. The magnetisation curves of the quasi-crystalline alloys below a critical temperature T_C of the order of 120 K show both ferromagnetic and paramagnetic components. The former

saturates in fields of the order of 600 Oe and the saturation magnetisation at lower temperatures is of the order of 0.2 A m^2 kg^{-1}. The paramagnetic effective moment 0.3 μ_B/Mn is much smaller than the (1–2) μ_B typically reported for i-$Al_{80-y}Si_yMn_{20}$ with $y \simeq 6$ [4, 5]. These different results show that the question of the magnetism in crystalline and quasi-crystalline Al–Si–Mn alloys and which transition-metal sites are magnetic are still open questions.

Neutron diffraction, using contrast variation on the Mn sites [11], has been used to determine the atomic decoration in Al–Si–Mn quasi-crystals without reference to any specific model (except for the Bravais lattice, which was taken as a primitive hypercube in six dimensions) within the strip and projection formalism. The individual structure factors were calculated for the Al and Mn sites independently together with their phases [12]. Manganese atoms occupy the vertices of the Penrose tiles in three dimensions whereas (Al,Si) atoms are located on rhombic faces and on the triad axis of the prolate rhombohedron [13]. Occupancy of these latter sites is fractional, thus embodying the necessary chemical modulation to allow stability. The important point is that only very few complete Mackay icosahedra are still present in the quasi-crystalline structure, while most Mn atoms belong to triangular 'fragments' of this polyhedron, a figure that compares fairly well with the configuration found in β-Al_9SiMn_3.

We have studied the crystalline and icosahedral quasi-crystalline Al–Si–Mn alloys using Mössbauer effect (ME) spectroscopy on samples for which the Mn was isomorphically substituted with 28 at.% Fe [7]. The sign of the dominating electric field gradient (EFG) observed for the quasi-crystal was found to be the same as that found for the hexagonal phase, and differing from the result for the other crystalline phases (cubic and orthorhombic). This also points to a certain similarity in local atomic configuration between these two structures (this point will be discussed more fully elsewhere [14]). It was then very surprising to discover that the 28 at.% Fe substituted hexagonal phase undergoes a transition with a critical temperature $T_C \simeq 80$ K [8] since it is known that β-Al_9SiMn_3 does not order magnetically at least down to 4.2 K, and i-$Al_{74}Si_6Mn_{20}$ orders with a spin-glass transition at about $T_g \simeq 5$ K [4].

We present here results of different studies on the hexagonal alloy system β-$Al_{74}Si_6(Mn_{1-x}Fe_x)_{20}$. These include room-temperature x-ray diffraction and temperature-dependent neutron diffraction for $x = 0.28$, and magnetic susceptibility and ME studies for $x = 0.1$, 0.2 and 0.28. We conclude that the transitions found are of magnetic origin, and present a provisional magnetic phase diagram that is consistent with the known properties of this system.

2. Experimental details

The β-$Al_{74}Si_6(Mn_{1-x}Fe_x)_{20}$ (denoted β-$Al_9Si(Mn_{1-x}Fe_x)_3$) alloys have been prepared with melt spinning with $x = 0.1$, 0.2 and 0.28. The crystalline structure was checked by x-ray diffraction on a Siemens diffractometer using monochromatised Co Kα radiation. The diffraction results were evaluated using an automatic fitting program, which gives results on the positions for all lines found. These positions were compared with a table of angles and intensities calculated for the known hexagonal structure [1]. All significant lines have been indexed in this way, and the results are given for $x = 0.28$ in table 1. No important lines are missing and no further lines have been observed. The experimental line intensities show effects of crystalline texture typical for hexagonal systems.

Table 1. Results for the x-ray line positions 2Θ and intensities of the $x = 0.28$ sample (first two columns) compared to the theoretical lines ((*hkl*), 2Θ and intensity). Some experimental lines are shown with double indices due to overlap. The theoretical intensities have been normalised to the strongest intensity for (301). Since this line overlaps the (212) line in the experimental spectrum, this intensity has been arbitrarily normalised to the sum of (301) and (212) theoretical intensities.

Experimental		Theoretical		
2Θ (deg)	Intensity	(*hkl*)	2Θ (deg)	Intensity
15.771	871	(100)	15.81	814
20.662	295	(101)	20.69	63
26.638	427	(002)	26.70	188
27.539	246	(110)	27.57	44
31.105	264	(102)	31.18	76
31.835	182	(200)	31.97	28
34.676	324	(201)	34.72	126
38.673	148	(112)	38.76	34
42.053	150	(202)	42.10	33
42.642	163	(210)	42.69	41
43.656	750	(103)	43.76	337
44.861	163	(211)	44.90	52
48.724	480	(300)	48.75	237
50.855	1843	(301)	50.75	1000
		(212)	51.07	843
52.425	1340	(203)	52.51	614
54.881	350	(004)	55.01	132
56.400	255	(302)	56.45	108
56.894	428	(220)	56.92	169
57.485	160	(104)	57.62	71
60.252	44	(213)	60.32	19
61.174	118	(311)	61.23	51
65.067	152	(204)	65.04	21
		(303)	65.20	58
71.914	105	(214)	72.03	38
73.200	85	(402)	73.28	21
74.356	98	(313)	74.45	30
76.355	111	(304)	76.54	30
79.782	211	(411)	79.72	72
		(322)	79.97	89
80.971	80	(403)	81.12	18
83.012	75	(224)	83.15	22
87.508	546	(323)	87.66	212
		(006)	87.70	68
90.197	551	(305)	90.41	290
91.161	331	(330)	91.26	174
92.901	357	(502)	93.03	184
97.244	66	(332)	97.39	41
98.195	138	(324)	98.38	77
101.427	50	(511)	101.54	18
107.208	194	(423)	107.44	8
		(306)	107.48	110
112.739	154	(601)	112.91	116
114.212	209	(513)	114.41	136
116.441	210	(334)	116.65	140
117.147	156	(207)	117.24	36
		(415)	117.48	87
120.091	151	(521)	120.19	96

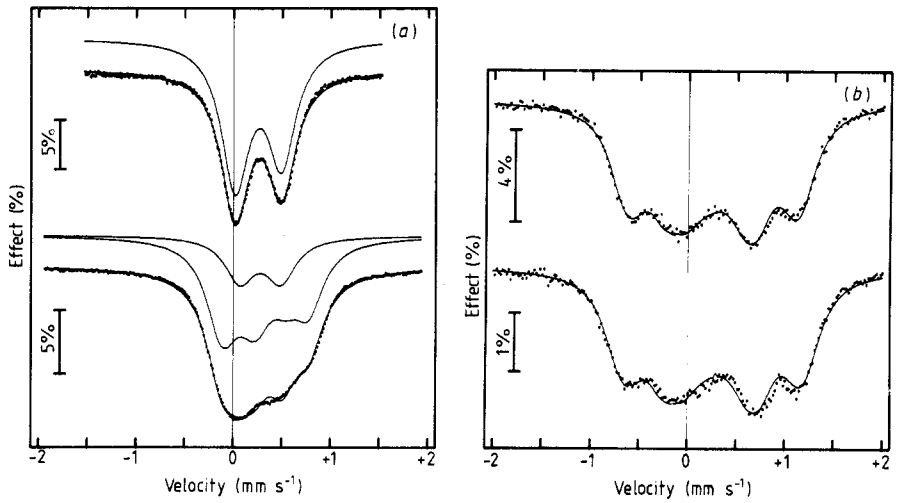

Figure 2. Mössbauer spectra for β-$Al_9Si(Mn_{0.72}Fe_{0.28})_3$. (*a*) Zero external field, with (upper) $T = 110$ K and (lower) $T = 4.2$ K. (*b*) In an external field of 5 T (perpendicular to γ-ray) for (upper) $T = 122$ K and (lower) $T = 4.2$ K. The fits are explained in the text.

Magnetic susceptibility measurements were performed on a calibrated Foner-type magnetometer. The neutron diffraction studies were made at the Institute Laue Langevin on the DIB two-axis diffractometer at $\lambda = 2.52$ Å. Details have been given elsewhere in similar (but high-temperature) neutron diffraction studies [13, 15].

The Mössbauer effect (ME) spectra were taken using a ^{57}Co–Rh source at room temperature. The spectra showing mixed hyperfine magnetic and quadrupole interactions have been treated using the exact Hamiltonian. There are two different cases for the direction of the hyperfine magnetic field B_{hf} within the principal axis system of the EFG. In the first case, it was assumed that there was no correlation between the EFG principal axes and the direction of the hyperfine magnetic field. The algorithm for calculating the spectrum form in this case has been given by Blaes *et al* [16]. In the second case, B_{hf} was considered fixed within the EFG principal axis system. The algorithm for calculating the spectrum form in this case has been given by Blaes *et al* [16]. In the second case, B_{hf} was considered fixed within the EFG principal axis system. The algorithm that we have used for calculating the spectrum was taken from a program written by Ruebenbauer and Birchall [17].

3. Results and discussion

The zero-field Mössbauer spectra at $T = 110$ and 4.2 K are shown for the $x = 0.28$ alloy in figure 2(*a*). The strong asymmetry in the first spectrum is due to crystalline texture typical of powders of hexagonal structures. The succeeding studies are made in magic-angle geometry to avoid this problem [7]. Obviously there is a change at low temperatures, but the resulting change in the spectrum is not large enough to enable us to distinguish clearly between the presence of magnetic splitting (non-zero magnetic hyperfine field B_{hf}), or a change in the EFG. This change has been followed as a function of temperature between 4.2 K and room temperature. By assuming that this change is

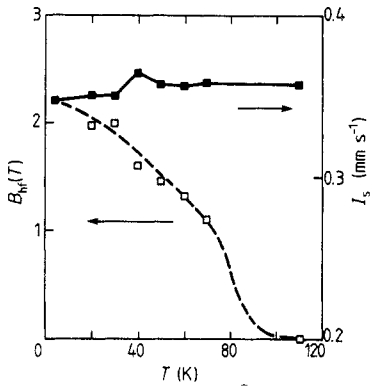

Figure 3. The evaluation of the spectra for β-$Al_9Si(Mn_{0.72}Fe_{0.28})_3$ under the assumption of a magnetic transition. The magnetic hyperfine field $B_{hf}(T)$ shows a transition near $T_C \simeq 80$ K. The isomer shift $I_S(T)$ shows no significant change near T_C.

related to a non-zero hyperfine field, we obtain the temperature dependence of B_{hf} shown in figure 3. Also shown is the associated isomer shift (referenced to BCC Fe at room temperature). The magnetic hyperfine field shows a transition at a critical temperature $T_C \simeq 80$ K. The saturation hyperfine field at $T = 0$ K is found by extrapolation to be $B_{hf}(0) \simeq 2.3$ T. From this value, and using the hyperfine coupling constant found in BCC Fe (34 T/2.3 μ_B), we estimate that the Fe saturation moments are about $\mu_{Fe} \simeq 0.15\ \mu_B$. We find that the low-temperature spectra could best be fit by assuming a fixed angle of $\theta = 90°$ and $\varphi = 0$ for the orientation of B_{hf} in the EFG principal axis system, and an asymmetry parameter of $\eta = 0.3$. A further improvement was possible by using two subspectra differing only in the value of B_{hf}: in one subspectrum $B_{hf} = 0$ was set. This yielded a fit with $\frac{1}{2}eQV_{zz} = -0.38$ mm s^{-1} and 75% of the area in the magnetic ($B_{hf} = 2.3$ T) and 25% in the non-magnetic subspectrum. We will return to this interesting point later in discussing the important role played by Fe–Fe pairs and triplets in the magnetic structure. This choice for θ and φ is not unique, so that the above values for η and $\frac{1}{2}eQV_{zz}$ are only estimations. In order to evaluate the saturation moment from the magnetic hyperfine field $B_{hf}(0)$, we have assumed a typical hyperfine constant found in many Fe-containing alloys. It seems that this proportionality between local iron moment and the hyperfine field is observed when the Fe majority band is not fully occupied [18].

In figure 2(*b*) we show spectra taken in an external field of 5 T directed perpendicular to the direction of the γ-ray direction. The spectrum taken at $T = 122$ K is from the paramagnetic state ($T > T_C$), and from this spectrum we obtain that the sign of V_{zz} is negative: $q = \frac{1}{2}eQV_{zz} = -0.45$ mm s^{-1}, $\eta = 0.9$ and $B_{int} = 4.7$ T. The lower spectrum at $T = 4.2$ K is very much below $T_C = 80$ K. Nevertheless, this spectrum yields a similar internal field of 4.9 T, $q = -0.46$ mm s^{-1}, and $\eta = 0.8$. This result is due to the fact that the hyperfine field $B_{hf} = 2.3$ T from the internal magnetic moments is oriented randomly with respect to the direction of the external field, so that, on average, the internal field is equal to the external field. This would no longer be the case if the external field could change the spin texture, or further polarise the small Fe magnetic moments. Thus only one component was used to evaluate this spectrum since the two components used for the zero-field spectrum would now have nearly the same internal field. The results from the spectrum at $T = 122$ K show that these conclusions hold as well near to T_C.

In order to distinguish a magnetic from a crystallographic transition, the sample β-$Al_9Si(Mn_{0.72}Fe_{0.28})_3$ was studied by neutron diffraction between room temperature (RT)

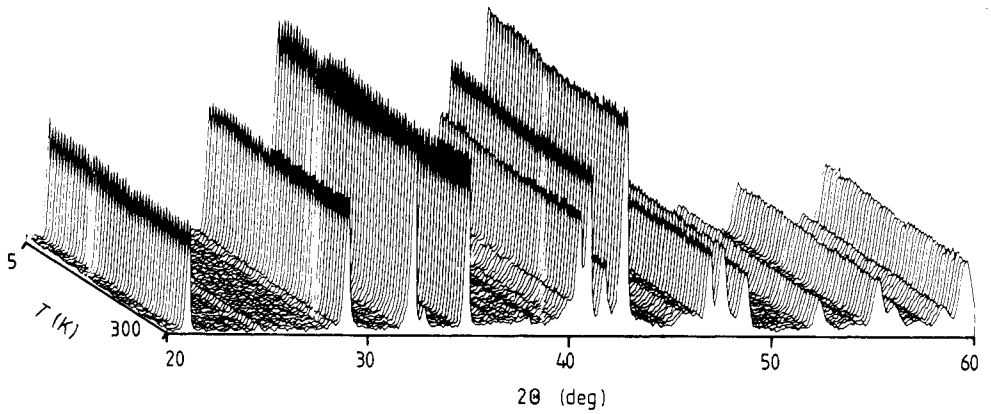

Figure 4. Neutron diffraction spectra ($\lambda = 2.52$ Å) at different temperatures between RT and 5 K. There is no change that could be associated with the transition at $T_C \simeq 80$ K.

and 5 K, similar to the diffraction studies on the quasi-crystalline samples above RT [12, 15]. The results of the 2Θ scans ($\lambda = 2.52$ Å) at different temperatures is shown in figure 4. Since, in this sample, the composition $x = 0.28$ had been chosen to yield a zero neutron scattering length for the transition-metal sublattice ($Mn_{1-x}Fe_x$) [12], these diffraction diagrams contain only the lines associated with the ($Al_{74}Si_6$) sublattice. However, any crystallographic phase transition at T_C would be expected to lead to changes in the low-temperature diffraction results as well. The absence of any such changes allows us to conclude that there is no change in structure at T_C, justifying the interpretation that the change in the Mössbauer spectra is indeed of magnetic origin. A sample of composition β-Al_9SiMn_3 was studied under the same conditions down to 1.5 K and showed no structural changes as well.

ME spectra for the $x = 0.1$ and 0.2 samples at low temperatures have been taken and they have been analysed in a similar way as for the $x = 0.28$ sample. Because of the lower ordering temperature, and smaller change in the spectra, T_C was determined simply by the change in the linewidth with decreasing temperature. The change in T_C with x is shown in figure 5(*a*). We see that T_C decreases approximately linearly with Fe concentration. The saturation hyperfine field at $T = 0$ K, $B_{hf}(0)$, is shown in figure 5(*b*). This has been estimated from the results at 4.2 K. As will be shown from the susceptibility results, there is a spin-glass transition at a lower temperature T_g. In the case of ferromagnetic to spin-glass magnetic double transitions, there is generally an increase in $B_{hf}(T)$ below T_g (see [19]). We neglect any such possible further increase in B_{hf}, so that the real values might be somewhat larger, especially for $x = 0.1$ and 0.2. $B_{hf}(0)$ decreases with decreasing x, indicating that, in the limit of infinite dilution, the Fe atom does not carry a magnetic moment. In fact, $B_{hf}(0)$ decreases faster with decreasing x than T_C does. One possible interpretation is that Fe–Fe pairs and triplets are very important in determining the magnetic properties of this system.

The magnetisation of the β-$Al_9Si(Mn_{0.72}Fe_{0.28})_3$ phase in an external field of 1 T is shown in figure 6 as a function of temperature between 10 and 250 K. When measuring M versus B at different temperatures, we observed a small ferromagnetic component M_F, which saturated in an external field of 0.3 T ($M_F = 4.6 \times 10^{-2}$ A m^2 kg^{-1}). This component has been found to be temperature-independent. If we assume M_F is due to

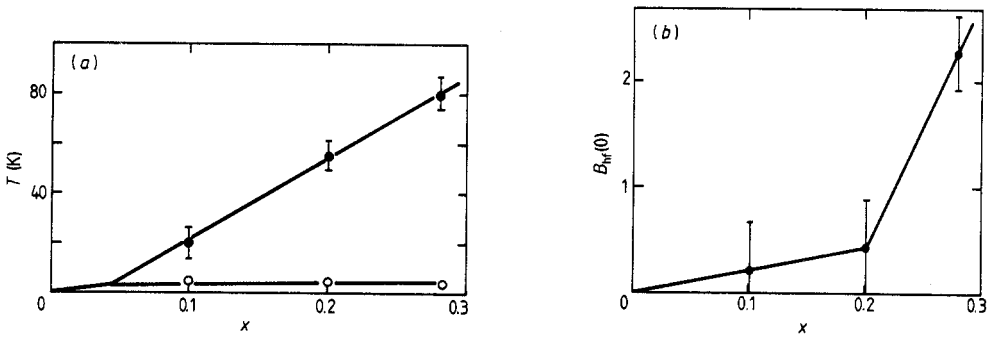

Figure 5. Dependence on the Fe concentration x of the (a) upper (T_C) and lower (T_g) transition temperatures as determined by Mössbauer spectroscopy (T_C) and magnetic susceptibility (both), and (b) the estimated saturation hyperfine field $B_{hf}(0)$.

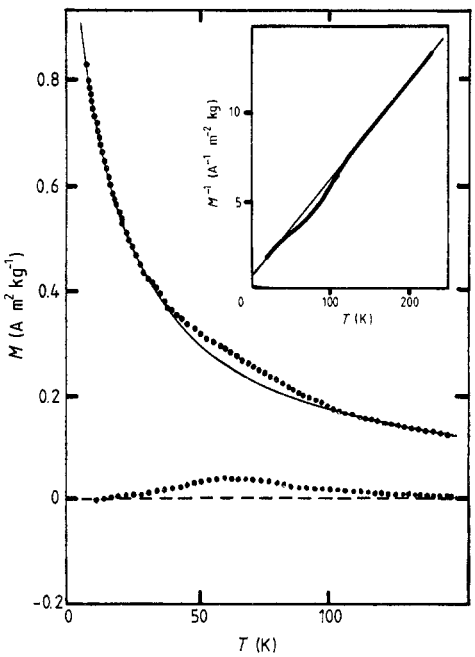

Figure 6. Magnetisation in an external magnetic field of 1 T of the sample β-$Al_9Si(Mn_{0.72}Fe_{0.28})_3$ over the range 10 to 250 K. The upper curve is compared to the Curie–Weiss form $M_{CW} = C/(T + \Theta)$ (shown as a thin full line) determined from the inverse plot (see inset). The difference M_{ex} is shown below. The maximum at 70–80 K is to be compared with the transition found in the Mössbauer hyperfine field (figure 4).

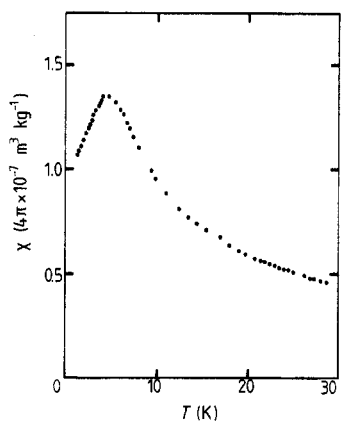

Figure 7. Susceptibility of the sample β-$Al_9Si(Mn_{0.80}Fe_{0.20})_3$ over the range 1.5 to 30 K. The maximum at $T_g \simeq 4$ K is associated with a spin-glass transition. Below T_g the susceptibility has been measured by an AC technique. Above T_g the initial slope of the magnetisation has been reported. The transition temperature T_g for different samples is relatively constant, as shown in the lower part of figure 6(a).

undissolved Fe small particles, this ferromagnetic component would only involve a very small fraction of the total Fe content (we estimate 0.2%). M_F has therefore been subtracted from the measured magnetisation M_{meas}: $M = M_{meas} - M_F$. The remaining $M(T)$ shows Curie–Weiss behaviour down to about 5 K, with a broad deviation between 40 and 110 K. This Curie–Weiss component is very similar to that found in the QC phase [4]. By plotting $1/M$ as a function of T (see inset to figure 6), we have been able to estimate the Curie–Weiss component M_{CW} and find $M_{CW} = 18.5/(T + 12.5)$ (in units of A m^2 kg^{-1} at 1 T). The difference $M - M_{CW}$ is shown at the bottom of the figure as well. We observe a large broad maximum near 70–80 K with an excess magnetisation of about $M_{ex} = 3.5 \times 10^{-2}$ A m^2 kg^{-1} at 1 T. This maximum is associated with the transition at $T_C \simeq 80$ K observed in the Mössbauer spectra. Assuming an antiferromagnetic transition, we can obtain a rough idea of the magnitude of the magnetic moments contributing to this transition from the Curie susceptibility with $T = T_C$:

$$M_{ex} = \frac{p_{eff}^2}{3k_B T_C} \mathcal{N}$$

where $p_{eff} = g[S(S+1)]^{1/2}\mu_B$ is the effective moment, and $\mathcal{N}$ is the number of magnetic moments per gram. If we take for $\mathcal{N}$ only the magnetic Fe atoms as determined from the ME spectrum at 4.2 K, we find $p_{eff}(\chi) \simeq 1\ \mu_B$. From the Mössbauer results we have $\mu_{Fe} = gS\mu_B \simeq 0.15\ \mu_B$, leading to a prediction of $p_{eff}(ME) \simeq 0.3\ \mu_B$, which is somewhat smaller. Including all the Mn atoms in the magnetisation would decrease $p_{eff}(\chi)$ to about 0.5 μ_B. However, the existence of the background Curie–Weiss susceptibility component for $T < T_C$ contradicts this hypothesis, so that it seems that mostly only Fe moments are involved in this (upper) transition.

In all the samples investigated, the Curie–Weiss background susceptibility shows a spin-glass transition at a temperature T_g, as is shown in figure 7 for the $x = 0.20$ sample. For the $x = 0.10$ and 0.20 samples, the anomaly in the susceptibility at the upper transition temperature could not be detected due to the fact that it is so small. We have found that T_g does not depend very much on Fe concentration in the range investigated here, being about $T_g \simeq 4$ K for all these three concentrations. Thus we interpret the Mössbauer and susceptibility results as indicating a magnetic double transition. In the upper transition, it seems that mostly only the Fe moments are involved, and the transition is antiferromagnetic. In the lower transition, all moments are involved, and the transition is spin-glass.

The most interesting fact about the magnetic transition in the Fe-doped β-Al_9SiMn_3 is that it occurs at all. Both the cubic α-$Al_{16}Si_3Mn_4$ [20] and the hexagonal β-Al_9SiMn_3 [1] are constructed from (different) stacking sequences of Mackay icosahedra [21, 22]. For this reason, these two structures have been considered as the first approximation to the icosahedral quasi-crystal with concentration near i-$Al_{74}Si_6Mn_{20}$ [14, 22, 23]. In the hexagonal structure, there are two Mn nearest neighbours per Mn ion, which form triplets, as shown in figure 1(*b*). There are thus isolated Mn–Mn triplets in this structure. The cubic phase is non-magnetic with or without Fe substitution. There are two distinct Mn sites in this structure, in the ratio of 1 : 1. Preferential site substitution of Fe is known to occur, as we have previously shown [7], but there are no Mn–Mn nearest neighbours at either site. The QC i-$Al_{74}Si_6Mn_{20}$ with or without Fe substitution is weakly magnetic, with a Curie–Weiss-like susceptibility and a spin-glass ordering temperature near 4–5 K. From neutron scattering using contrast variation, Janot *et al* [12, 13, 15] have shown that the local configuration around the Mn atom is similar to that found in the cubic and

hexagonal systems, and there are no significant numbers of Mn–Mn pairs as nearest neighbours. The weak magnetism of the Fe-doped QC has little measurable effect on the ME spectra at 4.2 K in zero field or in an applied field [7].

These properties of α-AlSiMn and i-$Al_{74}Si_6Mn_{20}$ indicate that the magnetic behaviour of Fe-substituted β-Al_9SiMn_3 is most certainly due to the existence of the Fe–Fe pairs and triplets possible in this structure. As we have $(Mn_{1-x}Fe_x)$, if Mn and Fe are distributed at random, there will be a fraction of Fe atoms with at least one Fe NN given by $x(2-x)$, which for $x = 0.28$ is equal to 0.48, or about 50%. Presumably then only the Fe pairs and triplets carry a magnetic moment, and then longer-ranged interactions will lead to the observed magnetic order. In the low-temperature limit, this magnetic order also involves the Mn atoms, and is of spin-glass type. The ME spectrum at $T = 4.2$ K also indicates that only about 75% of the Fe atoms are magnetic at low temperatures. This is more than the predicted 50% Fe atoms in pairs and triplets. However, the spectrum was taken at low temperature, near the transition to the spin-glass state. Both the magnetic and the non-magnetic Fe atoms have the same EFG and isomer shift (the quadrupole spectrum above T_C shows no enlargement or other trace of a second site).

From figure 1(*b*) for the Mn first and second NN, we see that a realistic physical description of the magnetic interactions must include at least two different exchange constants. We denote J_1 as that between Fe NN, and J_2 as that between Fe second NN. We will also assume that $|J_1| > |J_2|$. The magnetic phase diagram as a function of Fe concentration will then depend upon the signs of these two constants (as an approximation we will take Mn atoms as non-magnetic since without Fe substitution, the hexagonal phase is not magnetically ordered). For example, for antiferromagnetic (AF) $J_1 < 0$, pairs of Fe moments will tend to align antiparallel, and triplets will be frustrated. These triplets, when ordered magnetically, will most probably be canted in a non-collinear fashion. In the case of ferromagnetic (FM) $J_1 > 0$, both pairs and triplets of Fe moments will tend to order as clusters. The sign of J_2 will greatly influence the type of long-range order. From figure 1(*b*) we see that the second NN build triangular loops as well. Thus if J_2 is AF, frustration will develop whatever the sign of J_1. This leads to spin-glass order. There should be a region of AF order as well in this case. However, for AF J_2, the topological frustration leads to non-trivial degeneracy in the pure limit (all atoms with non-zero moment), so that the magnetic ground state is not simple to predict. This problem has recently been discussed by Henley [24]. The current view on spin-glass order has also been reviewed by Campbell [25]. From the fact that the upper transition is AF, we conclude that $J_2 < 0$, but the sign of J_1 is not certain.

4. Conclusions

From the low-temperature nuclear diffraction spectra, we have shown that the transition in β-$Al_9Si(Mn_{1-x}Fe_x)_3$ is not structural in origin. Magnetic susceptibility has shown that a broad maximum is associated with the transition temperature as determined by Mössbauer spectroscopy. A second transition to a spin-glass state was found at lower temperatures.

The dependence of the transition temperature on the Fe concentration has been determined, and a magnetic phase diagram for this system has been suggested. From the Mössbauer hyperfine results, it has been concluded that, in the limit of infinite dilution, the Fe atom does not carry a magnetic moment and that Fe–Fe nearest neighbours play an important role in determining the magnetic properties in this system.

Acknowledgments

Thanks are due to Mr P Weinland (Ecole des Mines, Nancy) for the preparation of the specimens. We thank Dr P Monod (Laboratoire de Physique des Solides, Orsay) for his help in the magnetisation measurements. We are grateful to the Institute Laue Langevin for the allocation of beam time on the DIB two-axis diffractometer. We would also like to thank M de Boissieu (Grenoble) for the use of figures 1(*a*) and (*b*).

References

[1] Robinson K 1952 *Acta Crystallogr.* **5** 397–403
[2] Bancel J M and Heiney P A 1986 *Phys. Rev.* B **33** 7917–22
[3] Taylor M A 1959 *Acta Crystallogr.* **12** 393–6
[4] Bellissent R, Hippert F, Monod P and Vigneron P 1987 *Phys. Rev.* B **36** 5540–3
[5] Hauser J J, Chen H S and Waszczak J V 1986 *Phys. Rev.* B **33** 3577–80
[6] Warren W W Jr, Chen H S and Espinoza G P 1986 *Phys. Rev.* B **34** 4902–5
[7] Le Caër G, Brand R A and Dubois J M 1987 *Phil. Mag. Lett.* **56** 143–51
[8] Le Caër G, Brand R A and Dubois J M 1988 *Hyperfine Interact.* **42** 943–6
[9] Hauser J J, Chen H S, Espinoza G P and Waszczak J V 1986 *Phys. Rev.* B **34** 4674–8
[10] Dunlap R A, McHenery M E, Srinivas V, Bahadur D and O'Handley R C 1989 *Phys. Rev.* B **39** 4808–11
[11] Dubois J M, Janot Ch and Pannetier J 1986 *Phys. Lett.* **115A** 177–81
[12] Janot Ch, Dubois J M and Pannetier J 1987 *Physica* B + C **146** 351–72
[13] Janot Ch, de Boissieu, Dubois J M and Pannetier J 1989 *J. Phys.: Condens. Matter* **1** 1029–48
[14] Brand R A, Le Caër G and Dubois J M 1990 *J. Phys.: Condens. Matter* submitted
[15] Janot Ch, Dubois J M and Pannetier J 1987 *Mater. Sci. Forum* **22–24** 329–44
[16] Blaes N, Fisher H and Gonser U 1985 *Nucl. Instrum. Methods* B **9** 201–8
[17] Ruebenbauer K and Birchall T 1979 *Hyperfine Interact.* **7** 125–33
[18] Eriksson O and Svane A 1989 *J. Phys.: Condens. Matter* **1** 1589–600
[19] Brand R A, Manns V and Keune W 1983 *Heidelberg Colloquium on Spin Glasses (Springer Lecture Notes in Physics 192)* ed J L van Hemmen and I Morgenstern (Berlin: Springer) p 79
[20] Cooper M and Robinson K 1966 *Acta Crystallogr.* **20** 614–7
[21] Mackay A L 1981 *Sov. Phys.–Crystallogr.* **26** 571–82 *(Kristallografiya* **26** 910–9)
[22] Gratias D 1988 *Du Cristal à l'Amorphe* ed C Godèche (Paris: Les Editions de Physique) p 83
[23] Brand R A 1987 *Nucl. Instrum. Methods* B **28** 398–416
[24] Henley C L 1989 *Phys. Rev. Lett.* **62** 2056–9
[25] Campbell I A 1987 *Hyperfine Interact.* **34** 505–13